Article ID: 1003－6326(2003)06－1367－04

Numerical simulation of iron/TiC ceramic tappet brazed with TiZrNiCu filler metal①

ZHANG Li-xia(张丽霞), FENG Ji-cai(冯吉才), LI Zhuo-ran(李卓然)
(National Key Laboratory of Advanced Welding Production Technology,
Harbin Institute of Technology, Harbin 150001, China)

Abstract: Maximum value of thermal stress and stress concentration zones of iron/TiC ceramic tappet during cooling were studied. The results show that when the temperature is 300 K, the maximum values of shear stress and tensile stress on iron/TiC ceramic interface both appear on the tip of TiZrNiCu/iron interface, so cracks always originate from TiZrNiCu/iron interface. Positive tensile stress on iron undersurface relaxes to the inner of iron and negative tensile stress on iron undersurface concentrates on the side of iron as the temperature declines, which leads to the origination of cracks on iron undersurface because of the alternation between positive and negative tensile stress.

Key words: numerical simulation; TiC ceramic; iron; brazing
CLC number: TG 404 **Document code:** A

1 INTRODUCTION

Recently, with the development of auto engines to the direction of high speed and power, the properties of the tappets used in auto engines become more and more important. So how to improve the wear resistance, fatigue resistance and oil storage of the tappets becomes a major project in the auto field. A new kind of compound tappet was studied in this paper. It was made of TiC ceramic, which was brazed on the wear surface of iron. This kind of tappet can make full use of good wear resistance of TiC ceramic and good toughness of metal. Fig. 1 shows the microstructure of this new kind of compound tappet.

There are many methods for joining ceramic with metal, such as brazing[1-7], diffusion bonding[8-11] and microwave welding[12, 13]. Brazing has become one of the main methods of bonding ceramic and metal in these years. However, it is difficult to obtain a high strength joint because of the mismatch of physical property between ceramic and metal, which always leads to shear stress concentration at the interface of ceramic and metal. In this paper, numerical simulation of iron/TiC ceramic tappet brazed with TiZrNiCu is studied, which provides a reference for brazing compound tappets.

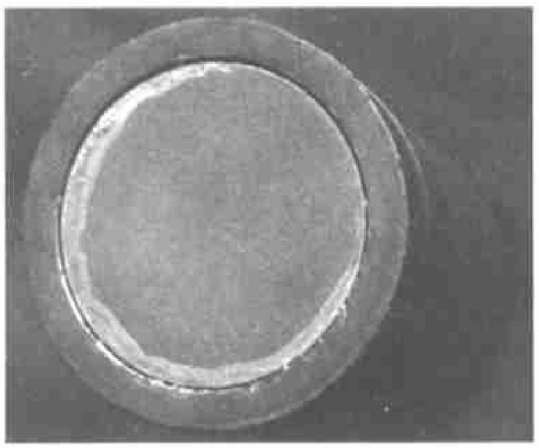

Fig. 1 Microstructure of compound tappet

2 RESULTS AND DISCUSSION

2.1 FEM model of iron/TiC ceramic tappet

Fig. 2 shows the two-dimensional FEM model of iron/TiC ceramic tappet. Two-dimensional size of test samples are as follows: that of iron is 40 mm × 75 mm; that of TiZrNiCu filler metal is 30 mm × 0.02 mm; and that of TiC ceramic is 30 mm × 5 mm. Table 1 shows the material parameters used in FEM calculation.

Two types of boundary condition are applied to the sample: 1) displacement boundary condition, which is applied to all nodes at iron undersurface($y=0$, $z=0$); 2) load boundary condition, which is applied to all nodes at TiC ceramic surface($F=4.8$ N).

When iron/TiZrNiCu/TiC ceramic joint is heated, TiZrNiCu filler metal becomes soft and thermal stress can be relaxed by the deformation of TiZrNiCu. Therefore, cooling course is only temperature-dependant during FEM calculation.

① **Foundation item:** Project(50175021) supported by the National Natural Science Foundation of China
Received date: 2003－02－08; **Accepted date:** 2003－06－12
Correspondence: ZHANG Li-xia, PhD; E-mail: zhanglxia@hit.edu.cn

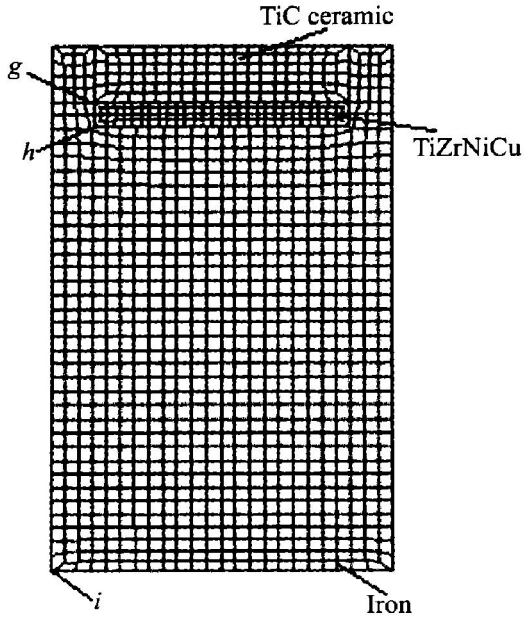

Fig. 2 Two-dimensional FEM model of iron/TiC ceramic tappet

Table 1 Material parameters used in FEM calculation

Material	Elastic modulus/GPa	Yield strength/MPa	Thermal expansion coefficient/$10^{-6}K^{-1}$	Poisson's ratio
TiC ceramic	103.5	250	11.76	0.250
Iron	310.0	240	9.76	0.326
TiZrNiCu	108.0	375	9.80	0.340

2.2 Effect of temperature on thermal stress

2.2.1 Effect of temperature on shear stress

Fig. 3 shows the development of shear stress during cooling along iron / TiC ceramic interface brazed at 1 173 K (Only left part of the tappet is considered because of its symmetry and element edges aren't erased for the convenience of analysis in this paper). Fig. 4 shows the change of shear stress at *g* point and *h* point during cooling. It can be seen from Fig. 3 and Fig. 4 that when the temperature declines, the shear stress on iron/TiC ceramic interface concentrates on the interface tip(*g* point and *h* point). When the temperature is 300 K, the maximum value of the shear stress is on left tip(*h* point) of TiZrNiCu/iron interface and cracks always originate from that site.

It also can be concluded from Fig. 3 and Fig. 4 that the shear stress value at *h* point decreases and then increases with declining temperature. The change of the shear stress value at *h* point is because that TiZrNiCu is soft at the beginning of cooling, which makes shear stress relax by its deformation and the shear stress value at *h* point decrease. Because TiZrNiCu can't deform any more after that course, the shear stress value on *h* point increases with declining temperature. When the temperature is 300 K, the maximum value of the shear stress of iron/TiC ceramic is up to 107.75 MPa.

2.2.2 Effect of temperature on tensile stress

Fig. 5 shows the development of tensile stress on iron/TiC ceramic interface during cooling. Fig. 6 shows the change of tensile stress at *g* point and *h* point during cooling. It can be seen from Fig. 5 and Fig. 6 that when the temperature declines, the tensile stress on the tip of TiC ceramic/TiZrNiCu interface decreases and then increases, while the tensile stress on the tip of TiZrNiCu/iron interface increases and then decreases. When the temperature decreases to 300 K , the maximum value of the

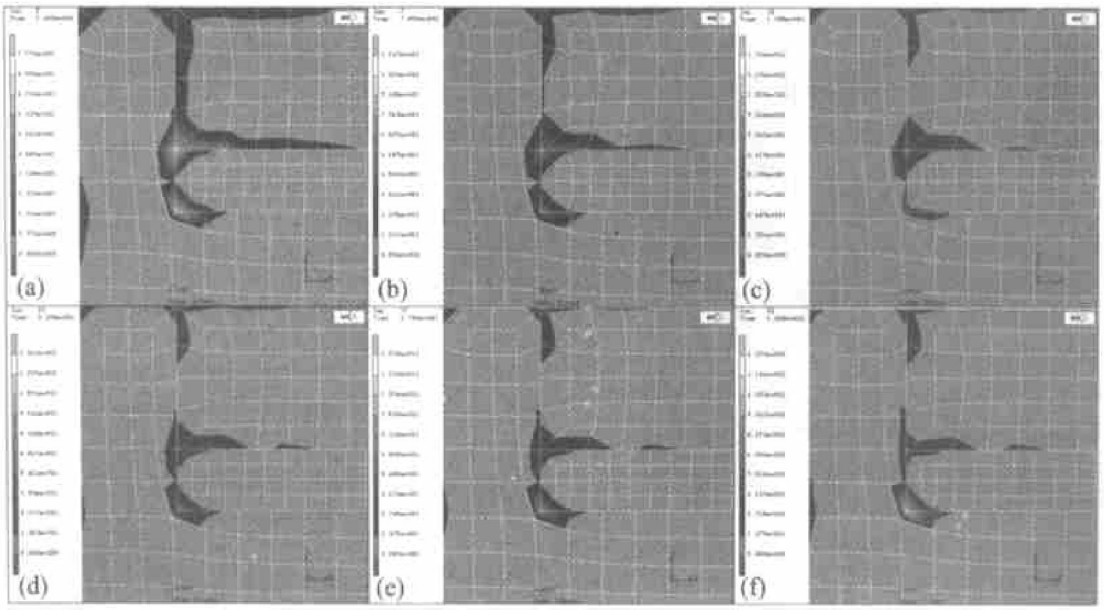

Fig. 3 Development of shear stress on left tip of iron/TiC ceramic interface during cooling (1173 K, v = 20 K/min)

(a) $-\Delta T$ = 44 K; (b) $-\Delta T$ = 61.6 K; (c) $-\Delta T$ = 132 K; (d) $-\Delta T$ = 281.6 K; (e) $-\Delta T$ = 325.6 K; (f) $-\Delta T$ = 440 K

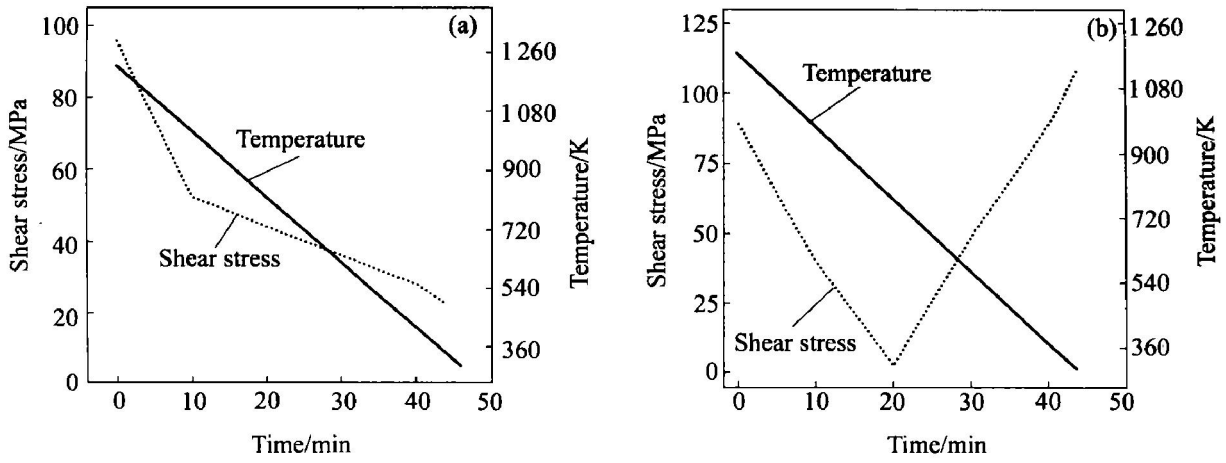

Fig. 4 Change of shear stress on different points during cooling (T = 1 173 K, v = 20 K/min)
(a) —g point; (b) —h point

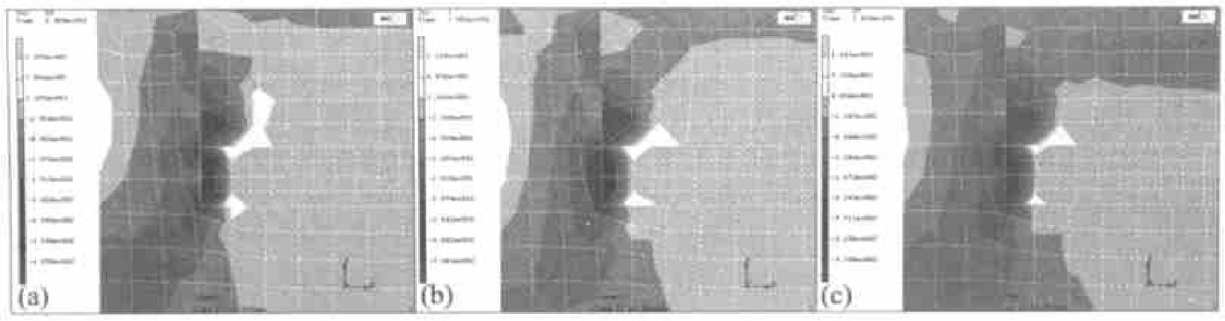

Fig. 5 Development of tensile stress on left tip of iron/TiC ceramic interface during cooling
(1 173 K, v = 20 K/min)
(a) —ΔT = 8.8 K; (b) —ΔT = 17.6 K; (c) —ΔT = 440 K

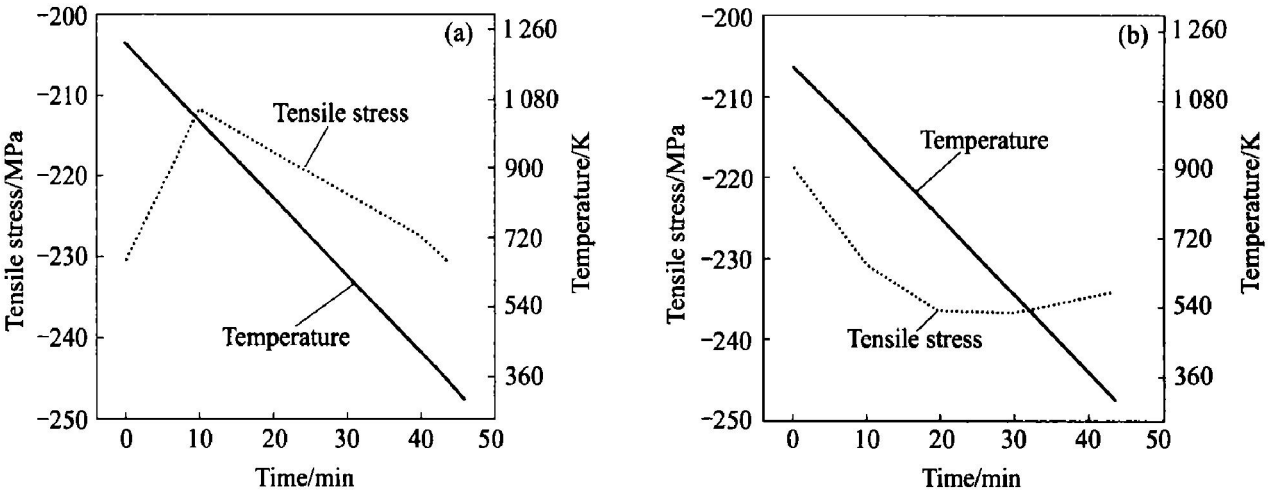

Fig. 6 Change of tensile stress on different points during cooling (T = 1 173 K, v = 20 K/min)
(a) —g point; (b) —h point

tensile stress on iron/TiC ceramic interface appears at h point and the value is − 234.072 MPa.

Fig. 7 shows the relaxation of positive tensile stress during cooling on left tip (i point) of iron undersurface. It can be seen from Fig. 7, when the temperature declines, positive tensile stress relaxation originates from the tip of iron undersurface and relaxes to the inner of iron.

Fig. 8 shows the concentration of negative tensile stress during cooling on left tip (i point) of iron undersurface. It can be seen from Fig. 8, following the relaxation course of positive tensile stress, negative tensile stress originates from and concentrates on the side of iron with declining temperature. Therefore, cracks on iron undersurface always take place because of the alternation between positive and negative tensile stress.

3 CONCLUSIONS

1) The maximum value of shear stress on ir

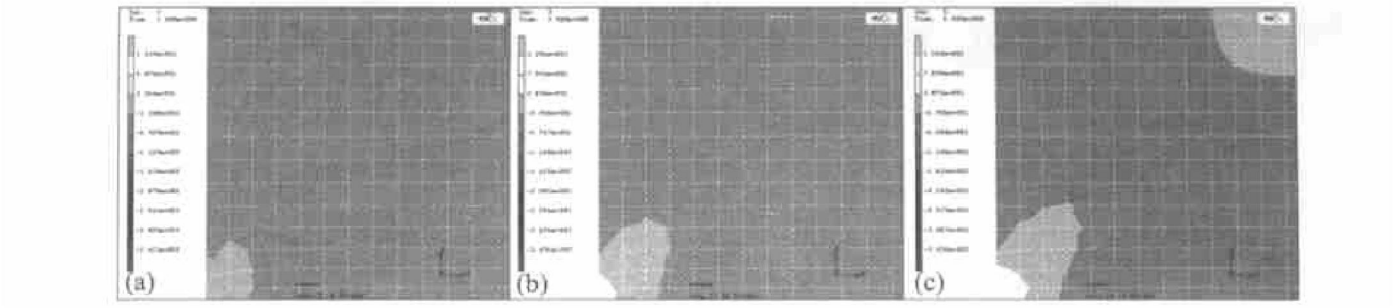

Fig. 7 Relaxation of tensile stress during cooling on left tip of iron undersurface (1 173 K, v = 20 K/min^{-1})
(a) $-\Delta T$ = 8.8 K; (b) $-\Delta T$ = 26.4 K; (c) $-\Delta T$ = 44 K

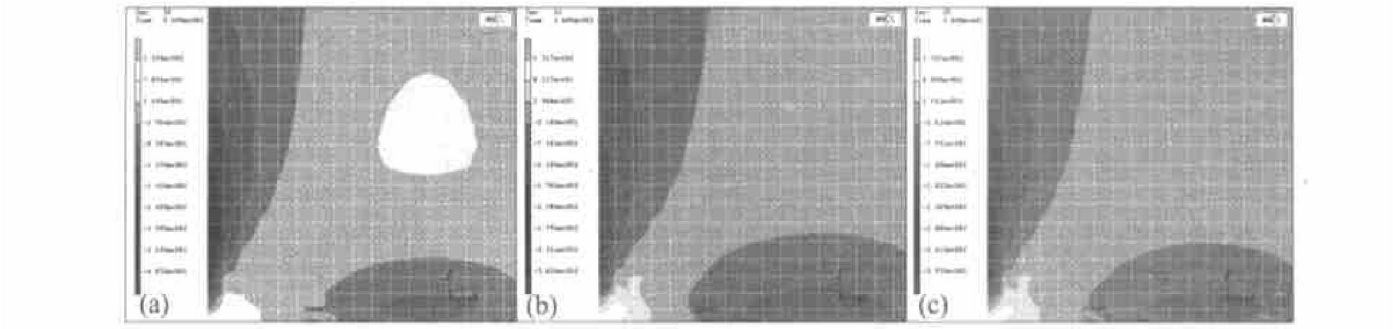

Fig. 8 Concentration of tensile stress during cooling on left tip of iron undersurface (1 173 K, v = 20 K/min^{-1})
(a) $-\Delta T$ = 228.8 K; (b) $-\Delta T$ = 316.8 K; (c) $-\Delta T$ = 440 K

ron/TiC ceramic interface is on the tip of TiZrNiCu/iron interface. The maximum value of shear stress decreases and then increases with declining temperature, which is up to 107.75 MPa when the temperature is 300 K.

2) The maximum value of tensile stress on iron/TiC ceramic interface appears on the tip of TiZrNiCu/iron interface. The maximum value of tensile stress increases and then decreases with declining temperature, which is up to − 234.072 MPa when the temperature is 300 K.

3) Positive tensile stress on iron undersurface relaxes to the inner of iron and negative tensile stress on iron undersurface concentrates on the side of iron with declining temperature.

REFERENCES

[1] LIU Hui-jie, FENG Ji-cai. The application and method of the bonding with ceramic and metal [J]. Welding and Joining, 1999(6): 5 - 9.

[2] Matsuo Y, Ito M, Tanignch M. Ceramic-metal joining for automobiles [J]. Industrial Ceramics, 1999, 19(3): 203 - 207.

[3] Zhang C G, Qiao G J, Jin Z H. Active brazing of pure alumina to Kovar alloy based on the partial transient liquid phase (PTLP) technique with Ni-Ti interlayer [J]. Journal of the European Ceramic Society, 2002, 22 (13): 2181 - 2186.

[4] Durov A V, Kostjuk B D, Shevchenko A V. Joining of zirconia to metal with Cu-Ga-Ti and Cu-Sn-Pb-Ti fillers [J]. Materials Science and Engineering, 2000, 290(1 - 2): 186 - 189.

[5] Bucklow I A. Development of a brazed ceramic-faced steel tappet [J]. The TWI Journal, 1995, 4(2): 260 - 308.

[6] Peteves S D. Joining nitride ceramics [J]. Ceramics International, 1996, 22(6): 527 - 533.

[7] Zhang C L, Shi K R, Guo Y. Improvement of Si_3N_4/40Cr steel joint strength by pressure brazing [J]. The Chinese Journal of Nonferrous Metals, 1999, 9(2): 283 - 289.

[8] Kliauga A M, Travessa D, Ferrante M. Al_2O_3/Ti interlayer/AISI 304 diffusion bonded joint: Microstructural characterization of the two interfaces [J]. Materials Characterization, 2001, 46(1): 65 - 74.

[9] Travessa D, Ferrante M, Den O G. Diffusion bonding of aluminium oxide to stainless steel using stress relief interlayers [J]. Materials Science and Engineering, 2002, 337(1 - 2): 287 - 296.

[10] Osendi M I, De P A, Miranzo P. Microstructure and mechanical strength of Si_3N_4/Ni solid state bonded interfaces [J]. Materials Science and Engineering, 2001, 308(1 - 2): 53 - 59.

[11] Abed A, Bin H P, Jalham I S, et al. Joining of Sialon ceramics by a stainless steel interlayer [J]. Journal of the European Ceramic Society, 2001, 21(16): 2803 - 2809.

[12] Siores E, Rego D D. Microwave applications in materials joining [J]. Journal of Materials Processing Technology, 1995, 48(1 - 4): 619 - 625.

[13] Yarlagadda P K D V, Soon R C T. Characterization of materials behaviour in microwave joining of ceramics [J]. Journal of Materials Processing Technology, 1998, 84(1 - 3): 162 - 174.

(Edited by YANG Bing)